Biosensors and Bioelectronics 142 (2019) 111553

Contents lists available at ScienceDirect

Biosensors and Bioelectronics

journal homepage: www.elsevier.com/locate/bios

Highly selective ratiometric electrogenerated chemiluminescence assay of DNA methyltransferase activity via polyaniline and anti-fouling peptide modified electrode

Yunxia Li, Lei Wang, Caifeng Ding*, Xiliang Luo**

Key Laboratory of Optic-electric Sensing and Analytical Chemistry for Life Science, MOE, Shandong Key Laboratory of Biochemical Analysis, Key Laboratory of Analytical Chemistry for Life Science in Universities of Shandong, College of Chemistry and Molecular Engineering, Qingdao University of Science and Technology, Qingdao, 266042, PR China

ARTICLE INFO

Keywords:
Hybridization chain reaction (HCR)
Ratiometric biosensor
Antifouling
Electrogenerated chemiluminescence (ECL)
DNA methyltransferase (MTase)

ABSTRACT

In this work, an antifouling electrochemiluminescent (ECL) ratiometric biosensor is designed for the accurate, selective and sensitive detection of DNA methyltransferase (MTase) activity based on a dual-signaling strategy. Briefly, an ITO electrode is used to construct the anti-fouling interfaces with the modification of polyaniline (PANI), AuNPs and peptide. Hairpin DNA molecules containing the symmetric sequence of 5′-CATC-3′ are attached onto the modified ITO electrode and the ds-DNA can be cut off in the presence of Dam MTase and DpnI. The residual DNA and two hairpin DNA could lead to the extension of ds-DNA due to the Hybridization Chain Reaction (HCR). ECL signal is amplified significantly with the insertion of PTC-NH_2 molecules into the dsDNA grooves. The $ECL_{PTC\text{-}NH2}/ECL_{Au@luminol}$ is found in a logarithmic linear relation with the concentration of Dam MTase. Moreover, owing to the presence of antifouling peptide on the sensing interface, the ECL biosensor was capable of sensing MTase activity in complex biological media, such as FBS samples and human serum with significantly reduced nonspecific adsorption effect. Assaying Dam MTase in complex sample mixture containing 5% calf serum and 5% human serum further proved the feasibility of this ECL biosensor for early clinical diagnosis.

1. Introduction

DNA methylation is a well-known epigenetic modification, playing a significant role in regulating gene expression and embryonic development (Heithoff et al., 1999; Robertson, 2005). In short palindromic sequences, DNA methylation occurs when the methyl transfers to cytosine or adenine from the donor S-adenosylmethionine induced by DNA methyltransferase (MTase) (Cheng and Roberts, 2001). Recent research reveals that different kinds of human diseases, such as colon cancer (Issa et al., 1993), gastric cancer (Mutze et al., 2011), lung cancer (Belinsky et al., 1996), and other diseases are associated with abnormal DNA methylation (Sheehan and Dorman, 2010; Coppieters et al., 2014). Thus, the DNA MTase has been used as predictive biomarker and potential therapeutic target. A variety of MTase activity assays have been developed for the early disease diagnosis and therapy. Traditional detection methods including gel electrophoresis (Rebeck and Samson, 1991), high performance liquid chromatography (Li et al., 2007a,b), and radioactive labeling (Bergerat et al., 1991), are time-consuming, complicated, requiring radio-active substance which is expensive and not efficient. To overcome the above drawbacks and improve the detection sensitivity, various strategies based on amplification and new technologies have been developed. Polymerase chain reaction (Van and Henikoff, 2000), bioluminescence (Jiang et al., 2012), chemiluminescence (Zeng et al., 2013; Luo et al., 2015), fluorescence (Li et al., 2010; Zhao et al., 2013), and electrochemical methods (Rauf et al., 2017; Chen et al., 2019; Gao et al., 2018), have been developed to detect DNA MTase activity in recent years.

Due to the excellent advantages, such as controllability, high sensitivity, and low-cost, electrochemiluminescence (ECL) has been attracting great attention in biological analysis especially in the detection of DNA MTase (Guo et al., 2018; Sun et al., 2017; Jiang et al., 2017; Zhou et al., 2016; Chen et al., 2018). It is noteworthy that, though with low detection limit, there is still a severe challenge to apply these ECL assays in real clinical application because the nonspesific adsorption

* Corresponding author. College of Chemistry and Molecular Engineering, Qingdao University of Science and Technology. Qingdao 266042, PR China.
** Corresponding author. College of Chemistry and Molecular Engineering, Qingdao University of Science and Technology. Qingdao 266042, PR China.
E-mail addresses: dingcaifeng2003@163.com (C. Ding), xiliangluo@qust.edu.cn (X. Luo).

https://doi.org/10.1016/j.bios.2019.111553
Received 17 March 2019; Received in revised form 25 July 2019; Accepted 29 July 2019
Available online 30 July 2019
0956-5663/

and interference in a complex background. To avoid the nonspecific protein adsorption, many efforts have been devoted to develop an antifouling sensing surface. Poly(ethylene glycol) (PEG) and oligo(ethylene glycol) (OEG) are the two of the most widely used antifouling materials owing to their surface hydration (Ladd et al., 2009; Luo et al., 2014; Vaisocherová et al., 2015; Prime and Whitesides., 1991; Callow and Callow., 2011; Liu et al., 2014a,b; Nowinski et al., 2012; Hui et al., 2017). But PEG and OEG have a tendency to be oxidized under oxidative condition that has limited their utility for long-term applications. (Knowles et al., 2017; Ran et al., 2014; Asuri et al., 2007). Another kind of conventional anti-fouling materials are arezwitterionic polymers, such as poly(sulfobetainemethacrylate) and poly(carboxybetainemethacrylate) whose synthetic processes are time-consuming and complicated. Peptides are natively zwitterionic, hydrophilic, and exhibit outstanding biocompatibility because of the formation of deprotonated carboxyl groups and protonated amine groups. Moreover, the synthetic process is considerably quick and convenient. With these merits, peptide has become a prospective candidate as an anti-fouling materials. A range of peptide-based antifouling films have been reported (Yang et al., 2017; Cui et al., 2017; Wu et al., 2017a,b; Chen et al., 2009; White et al., 2012; Liu et al., 2018; Wang et al., 2017, 2018; Hui et al., 2017; White et al., 2012).

In recent years, ratiometric ECL technology has attracted particular attention duo to its good performance in detection such as the low detection limit, high accuracy and reproducibility (Shao et al., 2016; Huo et al., 2018; Chen et al., 2012). In this work, we developed a new ECL ratiometric sensing surface with high ECL emission and sensitivity to DNA MTase activity as well as enhanced antifouling capability of a novel designed peptide (DKDKDKDPPPPC) with the excellent electrochemical activity of PANI. The electrode was incubated with Dam MTase which was used to catalyze the methylation reaction. When the recognition of DpnI was activated, it could cut off the ds-DNA. The remaining DNA could react with two hairpin DNA to form ds-DNA polymers, allowing the insertion of PTC-NH_2 to achieve universal detection of Dam MTase. This method could realize the detection of MTase activity with highly sensitive and selectivity.

2. Experimental section

2.1. Reagents and materials

Tris (2-carboxyethyl) phosphine hydrochloride solution (TCEP, 0.5 M) was purchased from Nanjing Chemical Reagent Co., Ltd. Aniline, chloroauric acid ($HAuCl_4$), luminol, bovine serum albumin (BSA) and 1-ethyl-3-(3-(dimethylamino)propyl) carbodiimide (EDC) were purchased from Sigma-Aldrich. Potassium persulfate ($K_2S_2O_8$), sulfuric acid (H_2SO_4, 95.0–98.0%), and hydrogen peroxide (H_2O_2, 30%) were purchased from Chengdu Kelong Chemical Reagent Co. (Chengdu, China). Indium Tin Oxide (ITO) coated glass slides were obtained from NanoSci Inc. (China). Hela cells and Raw cells were purchased from KeyGEN BioTECH Co. (China). DMEM medium, Fetal Bovine Serum and penicillin-streptomycin were obtained from HyClone Co. (China). Dam MTase, M.SssI MTase, HpaII MTase, and DpnI were purchased from New England Biolabs. Peptides and DNA oligonucleotides were purchased from Shanghai Sangon Biological Engineering Technology & Services Co. (China). The peptides and aptamer H_1, H_2, H_3 have the sequences as follows:

DKDKDKDPPPPC.
5′-HOOC-TTTTTGAAGGAGGGGCGATCTTTTTGATCTTTTT-$(CH_2)_6$-SH-3'.
5′-GGGGCGATGAAACTCGCCCCTCCTTC-3'.
5′-GTTTCATCGCCCCGAAGGAGGGGCGA -3'.

2.2. Apparatus

ECL emission was performed on a model MPI-E ECL analyzer (Xi'an Remex Electronics Co. Ltd., Xi'an, China). Cyclic voltammetric (CV) and Electrochemical impedance spectra (EIS) results were obtained on a CHI 660C electrochemical workstation (Shanghai CH Instruments, China). All electrochemical experiments were recorded with a three-electrode system: ITO electrode (working electrode), Ag/AgCl (saturated with KCl, reference electrode), and platinum wire (auxiliary electrode). The scanning electron images were recorded with Scanning Electron Microscope (SEM, S-4800, Hitachi). The Transmission Electron Micrographs (TEMs) were obtained using a JEOL-JEM 200 CX TEM instrument (Hitachi Instrument, Japanese). The fluorescence image is captured using TCS SP5 confocal laser microscope (Leica, Germany).

2.3. Synthesis of AuNPs, Au@luminol and PTC-NH_2

The AuNPs were synthesized by the reduction of gold hydrochlorate in aqueous solution according to classic method with slight modification (Lin et al., 2006). In short, sodium citrate (1.5 mL, 1%) was added into 50 mL $HAuCl_4$ (50 mL, 0.01%) boiling solution with continuous heating for 50 min. Then the colloidal suspension was left with siring to cool down to room temperature.

The Au@luminol nano-hybrids were prepared by the reduction of gold hydrochlorate with luminol in aqueous solution according to the method reported previously (Cui et al., 2010). In brief, 1.6 mL of 0.01 M luminol was added into 100 mL boiling HAuCl4 solution (0.01%, w/w) under vigorous stirring. After the solution was kept boiling for 30min, it turns from yellow to wine-red. The Au@luminol solution was left to cool down and then stored at 4 °C.

The amino-terminated perylene derivative (PTC-NH_2) was achieved according to the reported procedures (Lei et al., 2015). First, PTCDA (0.20 g) was dissolved in acetone solution (5 mL). Then, anhydrous ethylenediamine (0.5 mL) was added into the mixed solution under stirring at 4 °C. Next, the product was rinsed till pH 7.4. Finally, the product was dispersed with deionized water and stored at 4 °C for further use.

2.4. Preparation of Au@luminol − H_1 probes

Initially, the Au@luminol was centrifuged (1200 rcf, 10 min) to obtain red precipitation. Meanwhile, 35 μL of H_1 (100 nM) and 15 μL TCEP (10 mM) were mixed and incubated at room temperature 0.5 h to activate thiol. Then, the activated H_1 was added to the Au@luminol solution and incubated for 4 h at room temperature. The as-prepared mixture was centrifuged (10000 rcf, 5 min), and the red precipitates were resuspended with 300 μL of phosphate buffered saline (PBS, 0.01 M, pH 7.4). Then 75 mM EDC were added to the Au@luminol-H_1 solution to activate the carboxylic groups (37 °C, 1.5 h).

2.5. Fabrication of ratiometric ECL biosensor

The ratiometric ECL system for detecting DNA methyltransferase is illustrated in Scheme 1. First, PANI was electrodeposited onto the ITO electrode in 0.5 M H_2SO_4 solution containing 0.5 M aniline. The electrodeposition was performed by CV with scanning ranging from −0.2 V to +0.8 V at 100 mV s^{-1}. Next, 100 μL AuNPs suspension was dropped onto the sensing areas of PANI modified electrode for 30 min at 25 °C. The modified electrode was incubated 24 h in Phosphate Buffered Saline (PBS, 0.2 M, pH 7.4) containing 2.0 mg mL^{-1} multifunctional peptide. The peptides were immobilized on the modified electrode via Au–S bonds between the cys-terminal thiols and AuNPs. Then EDC activated Au@luminol-H_1 (20 μL) was added to the surface of the modified electrode and the Au@luminol-H_1 was linked to peptide via amide bond. Finally, the as-prepared sensing biosensor was cleaned with PBS buffer (0.1 M, pH 7.4) for subsequent tests.

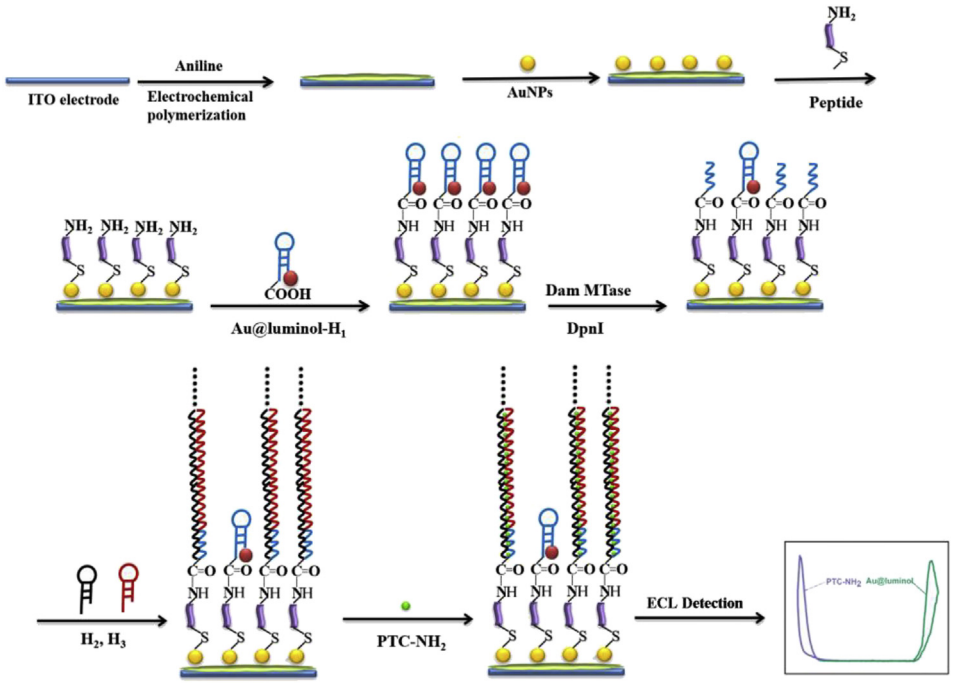

Scheme 1. Schematic illustration of the ratiometric ECL signal system.

2.6. ECL detection of dam MTase activity assay

Peptide functionalized sensing biosensor was incubated with 30 μL Au@luminol-H_1 (1×10^{-6} M) solution for 4 h at 37 °C. Then electrode was further incubated with buffer solution containing SAM and various amounts of Dam MTase for 2 h at 37 °C. Subsequently, 10 μL solution containing buffer and Dpn I was dispensed on the electrode and incubated for 2 h at 37 °C. Next, the prepared electrodes were incubated with a mixture of 5 μL hairpin probe H_2 (1 μM) and 5 μL hairpin probe H_3 (1 μM) for another 2 h. After that, 10 μL 2 mM PTC-NH_2 was dripped on the modified electrode and incubated for 7 h. Finally, ECL intensity was measured in PBS solution (0.1 M, pH 7.5) containing 0.1 M $K_2S_2O_8$ and 6.5 mM H_2O_2 from −1.8 to + 0.8 V at the scan rate of 100 mV s^{-1}. The voltage of the photomultiplier tube (PMT) was set at 750 V.

3. Results and discussion

Scheme 1 shows the assembled procedure of the ratiometric ECL biosensor. First, the electrode is modified with PANI film and AuNPs. Then, the modified electrode is incubated in Phosphate Buffered Saline (PBS, 0.2 M, pH 7.4) solution containing 2.0 mg mL^{-1} peptide which was designed to be antifouling for 24 h to construct the anti-fouling interface. Owing to the presence of peptide in the sensing interface, the prepared ECL sensor was capable of decrease the nonspecific absorption for detecting MTase activity in complex samples. Subsequently, a hairpin DNA containing the symmetric sequence of 5′-GATC-3′ is attached to the modified ITO electrode through Au–S bond. With the bonding of hairpin DNA, the electrode is incubated inside Dam MTase solution, which catalyzes the methylation. When DNA sequence is methylated (5′-GAmTC-3′), DpnI is activated which enables it to cut off the ds-DNA. The residual DNA and two types of hairpin DNA lead to the extension of ds-DNA polymer on the electrode surface through HCR. The HCR-generated dsDNA polymer promotes intercalation of the ECL indicator PTC-NH_2 into the ds-DNA grooves, resulting in the significantly enhanced ECL signal output. Thus, the methylation corresponding to the MTase activity could be monitored and detection with high selectivity and sensitivity by this method.

3.1. Characterization of AuNPs and Au@luminol

The morphology and size of the obtained AuNPs and Au@luminol are characterized with Transmission Electron Microscopy (TEM). As shown in Fig. S1A in the Supplementary Materials, the size distribution of the prepared AuNPs is 11–18 nm and the average diameter of which is about 15 nm. From Fig. S1B we can see that the size distribution of Au@luminol is 10–17 nm and Au@luminol displays an average particle size of 14 nm. Fig. S1C presents the UV–vis absorption of luminol with two peaks at around 300 and 360 nm (curve a), and the absorption peak of AuNPs is 525 nm (curve b). Compared to the spectrum of AuNPs, Au@luminol (curve c) exhibits absorption band at 365 and 530 nm, which is consistent with that reported (Cheng et al., 2014), indicating the successful preparation of Au@luminol.

3.2. Feasibility of ratiometric ECL biosensor

To confirm the feasibility of the approach, the ECL of PTC-NH_2 and Au@luminol nanoprobes are characterized separately. As shown in Fig. S2A and S2B, a cathode ECL emission peak of PTC-NH_2 nanoprobe is observed at −1.8 V, and an intense anode ECL emission peak of Au@luminol nanoprobe is observed at +0.8 V. To characterize ECL of the two nanoprobes within one potential scanning, ECL emissions of both luminol and Au@luminol are simultaneously detected. As can be seen from Fig. S2C, two well separated ECL signals appear during one potential scanning, and no additional emissions are found. Such results demonstrate that the as-prepared PTC-NH_2 and Au@luminol nanoprobes could be used as indicators simultaneously in one measurement.

3.3. Characterization of the developed biosensing interfaces

The surface morphology of sensing interface is characterized step-by-step with SEM. Fig. S3A is the surface of bare ITO electrode. Compared to bare ITO, Fig. S3B shows a network structure on the ITO electrode surface, revealing successful electro-deposition of PANI onto the patterned ITO electrode. In Fig. S3C, some spherical particles are found coated on the surface of PANI, and this suggests that AuNPs are assembled onto the PANI surface. These results demonstrate the

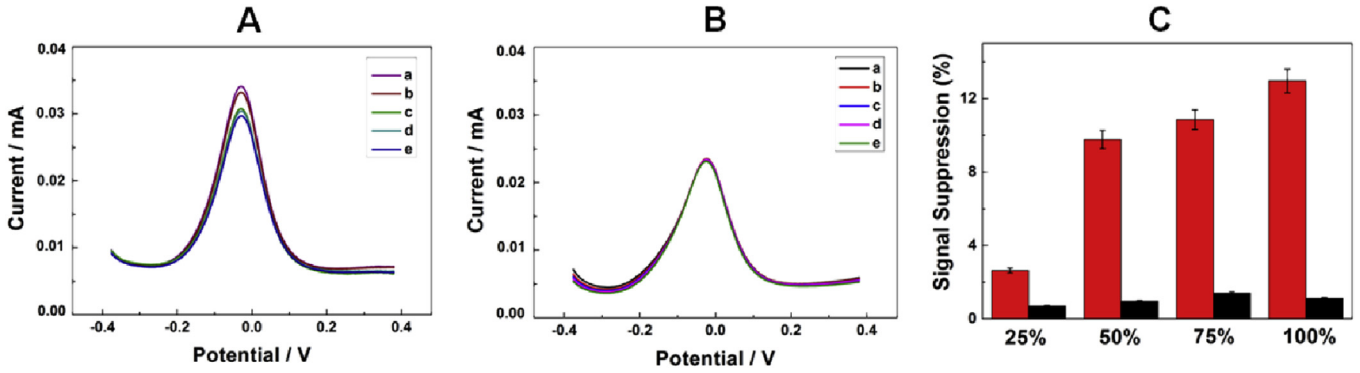

Fig. 1. DPV responses of PANI/ITO (A) and peptides/AuNPs/PANI/ITO (B) before and after incubated in various FBS (0%, 25%, 50%, 75%, 100%) samples. Antifouling property of the PANI/ITO (red) and peptides/AuNPs/PANI/ITO (black) for various concentrations of FBS samples(C). (For interpretation of the references to colour in this figure legend, the reader is referred to the Web version of this article.)

successful modification of ITO electrode.

3.4. Characterization of the antifouling ability

The Differential Pulse Voltammetry (DPV) is used to assess the antifouling ability of the peptide-based biosensor interfaces. Fig. 1A and Fig. 1B are the DPV responses of PANI and peptide/PANI modified ITO electrode after incubated in various concentrations of FBS (V/V). As can be seen in Fig. 1C, the DPV signals of the peptide/PANI modified electrode varies less than 2% even incubated in 100% FBS. This result demonstrates the good antifouling ability of the peptide-based biosensor interface, which is further verified by fluoresceinc diacetate (FDA) labeled cells (Fig. 2). Due to the better biocompatibility of PANI and AuNPs, there are more cells can be seen on the PANI/ITO and AuNPs/PANI/ITO electrodes than on the bare ITO electrode. Compared to PANI modified electrode and AuNPs/PANI modified electrode, only a few cells are observed at the peptide surface.

Hydrophilicity of the newly designed peptide modified biosensing interfaces is evaluated with static sessile drop method. As shown in Fig. S4 and Table S1, the bare ITO electrode, PANI modified electrode, AuNPs/PANI modified electrode, and peptide/AuNPs/PANI modified electrode present the water contact angle of (73.7 ± 3.0) °, (53.7 ± 2.8)°, (42.9 ± 2.4)°, and (16.1 ± 1.1)° respectively. Such results suggest good hydrophilicity of the peptide-functionalized sensing interfaces.

3.5. Electrical characterization of stepwise fabrication of ECL-sensing platform

The fabricated biosensor is characterized by Cyclic Voltammetry (CV) and Electrochemical Impedance Spectrum (EIS) step by step with the assembled process in PBS (0.1 M, pH 7.4) containing 5.0 mM $[Fe(CN)_6]^{4-/3-}$ and 0.1 M KCl. A pair of typical redox peaks of ferricyanide ions are observed at 0.13 V and 0.38 V on bare ITO electrode (Fig. S5A, curve a). The redox peak current increases in turn with the electropolymerization of PANI (Fig. S5A curve b) and modification with AuNPs (Fig. S5A curve c), which is attributed to the increase of the active surface area on the electrode. After the electrode surface is modified with peptide (Fig. S5A curve d) and Au@luminol (Fig. S5A curve e), the peak currents decrease in turn; and this is a result of the electron inert nature of the biomolecules. When Dam MTase and DpnI (Fig. S5A curve f) are introduced, the peak currents increase slightly. With the capture of hairpin DNA H_2, H_3 and intercalated probe PTC-NH_2 (Fig. S5A curves g, h), peak current decreases gradually, which is due to the electron inert nature of DNA and probe. The corresponding EIS spectra are shown in Fig. S5B, when bare ITO electrode (curve a) is electropolymerized with aniline, the EIS of the PANI displays a lower Ret (curve b), which verifies that PANI is beneficial to electron transfer because the conducting polymer formed a porous network on the electrode surface as shown in Fig. S2B. When PANI/ITO is modified with AuNPs, the R_{et} decreases, and this implies that the AuNPs have adsorbed at PANI surface. The diameter of semicircle increases when incubated with peptide (curve d) and Au@luminol-H_1 (curve e), which

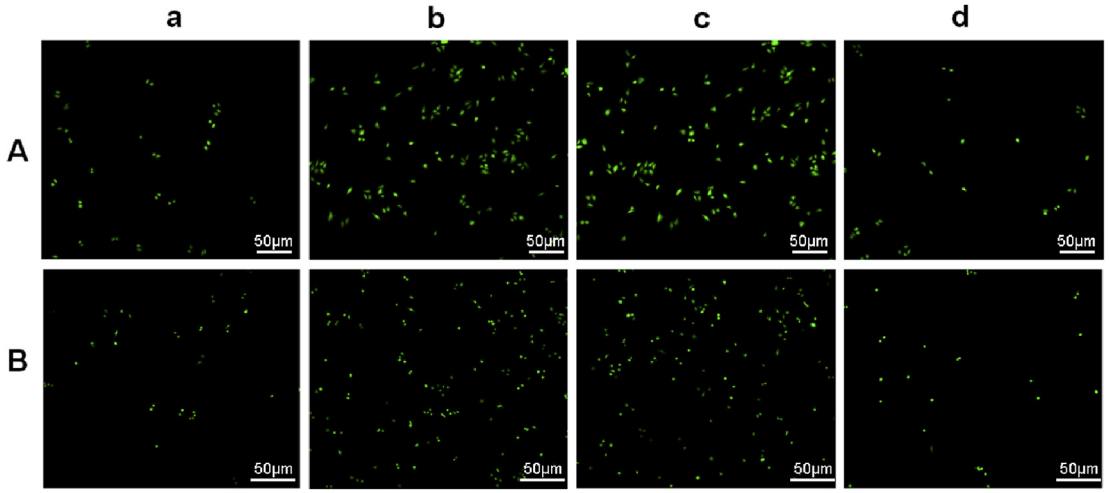

Fig. 2. Fluorescence images of HeLa cells (A) and Raw cells (B) incubated on (a) bare ITO electrode, (b) PANI/ITO electrode, (c) AuNPs/PANI/ITO electrode and (d) peptide/AuNPs/PANI/ITO electrode.

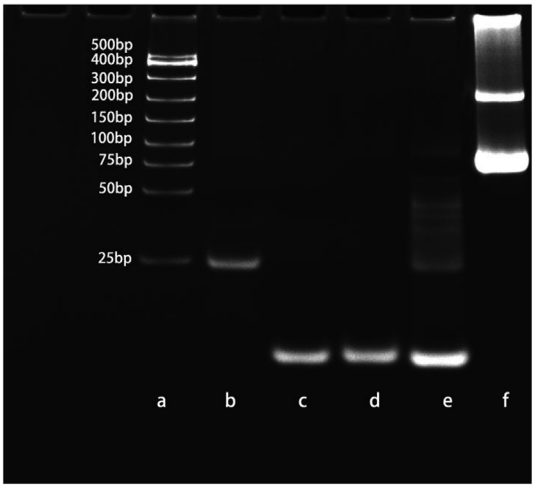

Fig. 3. PAGE analysis of marker (a), 5 μL hairpin DNA H_1 (10^{-6} M) (b), 5 μL hairpin DNA H_2 (10^{-6} M) (c), 5 μL hairpin DNA H_3 (10^{-6} M) (d), mixture of 5 μL hairpin DNA H_1 (10^{-6} M), 5 μL hairpin DNA H_2 (10^{-6} M) and 5 μL hairpin DNA H_3 (10^{-6} M) (e), mixture of 5 μL hairpin DNA H_1 (10^{-6} M), 5 μL hairpin DNA H_2 (10^{-6} M) and 5 μL hairpin DNA H_3 (10^{-6} M) with Dam MTase and DpnI (f).

indicated the successful modification of peptide and hairpin DNA H_1. When Dam MTase, DpnI (curve f) are introduced, Ret increases slightly for the cleavage of hairpin DNA probe. When the electrode is modified with hairpin DNA H_2, H_3, and probe PTC-NH_2, an increase of R_{et} is observed (curves f, g, h) due to the electron inert nature of biomolecules and probes. All the above results suggest the successful construction of the multiplex sensor.

3.6. Gel electrophoresis

Gel electrophoresis is used to confirm the HCR reaction. As shown in Fig. 3, the first four lanes are the marker, hairpin DNA H_1, hairpin DNA H_2, and hairpin DNA H_3, respectively. Lane e is the mixture of hairpin DNA H_1, hairpin DNA H_2, and hairpin DNA H_3 without Dam MTase and DpnI. When target Dam MTase and DpnI were introduced into the hairpin DNA H_1, the HCR reaction between residual DNA and two hairpin DNA H_2 and H_3 started and a new bands of dsDNA polymers were obtained (f). These PAGE results demonstrate successful HCR amplification reaction.

3.7. Quantification of dam MTase

The multiplex biosensor is employed to quantify Dam MTase by using Au@luminol and PTC-NH_2 nanoprobes. As shown in Fig. 4A, the anodic ECL peak intensity at around +0.8 V decreases with the concentrations of Dam MTase while that of the cathode at around −1.8 V increases. The logarithm of ($ECL_{PTC\text{-}NH2}/ECL_{Au@luminol}$) in Fig. 5B is in good linear relationship with the logarithm of Dam MTase concentration wihtin 0.05–100 U·mL^{-1}. The linear relationship can be described as $\lg(ECL_{PTC\text{-}NH2}/ECL_{Au@luminol}) = 0.416\ \lg C_{dam\ MTase}$ (U·mL^{-1}) + 0.048 (R^2 = 0.993). Detection limit is calculated to be 0.02 U·mL^{-1} (S/N = 3), which is lower than that reported methods (Table S1) (Tian et al., 2012; Li et al., 2007a,b, 2010; Wang et al., 2013, 2015; Chen et al., 2018; Zhao et al., 2014).

3.8. Selectivity of the biosensor

To investigate the selectivity of the present sensing biosensor, effects of other enzymes on the ECL intensity at the biosensor are studied. M.SssI MTase and HpaII MTase are selected as interference enzymes. As the former can methylates the recognition sequence 5′-CG-3′ while the latter is the target sequence of 5′-GC-3′. As can be seen in Figs. 5 and 10 U·mL^{-1} Dam MTase could induce variations of ECL ratio, while M.SssI MTase and HpaII MTase at the same concentration show few effects compared to the blank sample. The ratio of the ECL signal of the mixture of the three enzymes is almost the same with the single Dam Mtase. These results clearly demonstrate that this ECL-sensing platform has satisfying specificity for Dam MTase.

3.9. Dam MTase activity assay in biological fluid

To investigate the practical application of the ECL immunosensor, the $ECL_{PTC\text{-}NH2}/ECL_{Au@luminol}$ is tested by detecting Dam MTase in complex sample mixtures containing 5% calf serum and 5% human serum. As shown in Fig. S6A and Fig. S6B, the more Dam MTase is added, the larger of the $ECL_{PTC\text{-}NH2}/ECL_{Au@luminol}$ is observed. The results suggest acceptable accuracy of our assay for quantifying Dam MTase in complex biological fluids.

4. Conclusion

In conclusion, an antifouling ECL ratiometric biosensor is constructed based on HCR amplification strategy. In the presence of Dam MTase and DpnI, ds-DNA was cut off and the residual DNA induce HCR reaction to form extended dsDNA polymers causing the insertion of numerous PTC-NH2 into the dsDNA grooves, resulting in significantly amplified ECL signal. The ECL intensity of Au@luminol decreases with the increasing of target Dam MTase while the ECL intensity of PTC-NH2 increases gradually in one potential scanning, resulting in a dual-signaling ECL ratiometric sensing approach for the accurate and sensitive detection of Dam MTase activity. In the constructed sensing interface, hydrophilic peptide exhibits resistance to nonspecific protein adsorption, making the ratiometric ECL biosensor can be used to assay Dam MTase in 5% calf serum and 5% human serum with satisfying accuracy and without suffering from biofouling, suggesting great potential for practical application.

Declaration of interest statement

We herein declare that we have no financial and personal relationships with other people or organizations that can inappropriately influence our work, and there is no professional or other personal interest of any nature or kind in any product, service and/or company that could be construed as influencing the position presented in, or the review of, the manuscript entitled. We also declare that the manuscript has been read and approved by all authors named out (Yunxia Li, Lei Wang, Caifeng Ding, and Xiliang Luo) and there are no other persons who satisfy the criteria for authorship but are not listed out.

CRediT authorship contribution statement

Yunxia Li: Data curation, Formal analysis, Writing - original draft. **Lei Wang:** Software, Writing - review & editing. **Caifeng Ding:** Conceptualization, Funding acquisition, Investigation, Methodology, Project administration, Supervision. **Xiliang Luo:** Conceptualization, Funding acquisition, Resources, Project administration.

Acknowledgements

The authors greatly acknowledge support from the National Natural Science Foundation of China (Grants 21375070, 21675093), and the Taishan Scholar Program of Shandong Province of China (Grant ts20110829), and the Project Fund for Shangdong Key R&D Program (2017GGX20121).

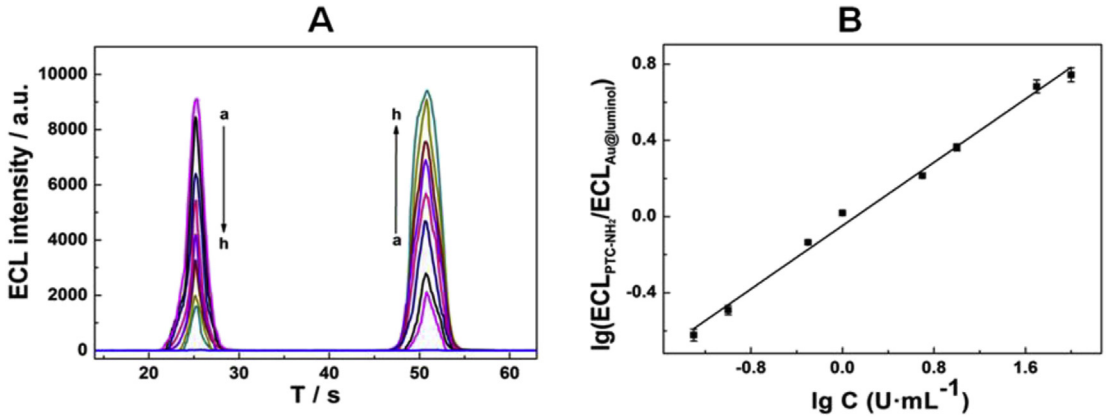

Fig. 4. (A) ECL intensity-time curves obtained on Au@luminol and PTC-NH_2 nanoprobes with Dam MTase concentration of 0.05, 0.1, 0.5, 1, 5, 10, 50, 100 U·mL^{-1} in air-saturated PBS buffer containing 0.1 M $K_2S_2O_8$, and 6.5 mM H_2O_2 at pH 8.0. (B) Linear calibration between Dam MTase concentration and the ratio of cathode to anode ECL peak intensity in PBS buffer containing 0.1 M $K_2S_2O_8$, and 6.5 mM H_2O_2 at pH 8.0.

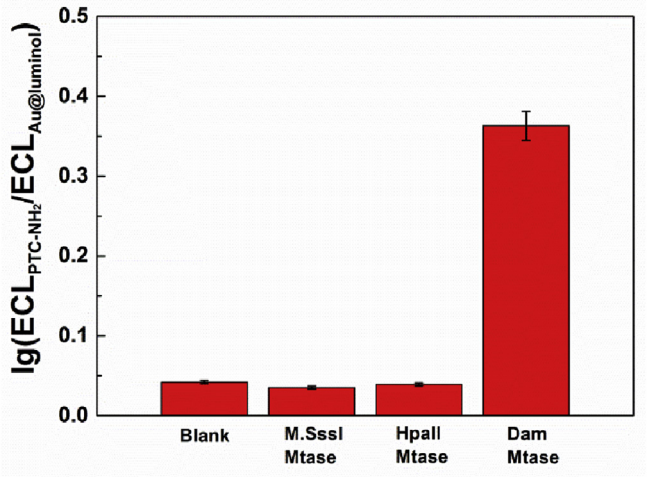

Fig. 5. Selectivity of the assay, enzyme concentration: 10 U·mL^{-1} each.

Appendix A. Supplementary data

Supplementary data to this article can be found online at https://doi.org/10.1016/j.bios.2019.111553.

References

Asuri, P., Karajanagi, S.S., Kane, R.S., Dordick, J.S., 2007. Small 3, 50–53.
Belinsky, S.A., Nikula, K.J., Baylin, S.B., Issa, J.P., 1996. P. Natl. Acad. Sci. USA. 93, 4045–4050.
Bergerat, A., Guschlbauer, W., Fazakerley, G.V., 1991. P. Natl. Acad. Sci. USA. 88, 6394–6397.
Callow, J.A., Callow, M.E., 2011. Nat. Commun. 2, 1–10.
Chen, S., Cao, Z., Jiang, S., 2009. Biomaterials 30, 5892–5896.
Chen, S., Lv, Y., Shen, Y., Ji, J., Zhou, Q., Liu, S., 2018. Acs Appl. Mater. Interface 10, 6887–6894.
Chen, Y., Meng, X., Gu, H., Yi, H., Su, W., 2019. Biosens. Bioelectron. 134, 117–122.
Chen, Y., Xu, J., Su, J., Xiang, Y., Yuan, R., Chai, Y., 2012. Anal. Chem. 84, 7750–7755.
Cheng, X., Roberts, R.J., 2001. Nucleic Acids Res. 29, 3784–3795.
Cheng, Y., Huang, Y., Lei, J., Zhang, L., 2014. Anal. Chem. 86, 5158–5163.
Coppieters, N., Dieriks, B.V., Lill, C., Faull, R.L., Curtis, M.A., Dragunow, M., 2014. Neurobiol. Aging 35, 1334–1344.
Cui, H., Wang, W., Duan, C.F., Dong, Y.P., Guo, J.Z., 2010. Chem. Eur J. 13, 6975–6984.
Cui, M., Wang, Y., Jiao, M., Jayachandran, S., Wu, Y., Fan, X., Luo, X., 2017. ACS Sens. 2, 490–494.
Gao, F., Fan, T., Ou, S., Wu, J., Zhang, J., Luo, J., Li, N., Yao, Y., Mou, Y., Liao, X., Geng, D., 2018. Biosens. Bioelectron. 99, 201–208.
Guo, Z., Qiao, B., Guo, Q., Zhang, H., Cai, C., Feng, J., 2018. Analyst 143, 3353–3359.
Heithoff, D.M., Sinsheimer, R.L., Low, D.A., Mahan, M.J., 1999. Science 284, 967–970.
Hui, N., Sun, X., Niu, S., Luo, X., 2017. ACS Appl. Mater. Interfaces 9, 2914–2923.
Huo, X.L., Zhang, N., Yang, H., Xu, J.J., Chen, H.Y., 2018. Anal. Chem. 90, 13723–13728.
Issa, J.P.J., Vertino, P.M., Wu, J., 1993. J. Natl. Cancer Inst. 85, 1235–1240.
Jiang, B., Yang, M., Yang, C., Xiang, Y., Yuan, R., 2017. Sens. Actuators B 247, 573–579.
Jiang, C., Yan, C.Y., Huang, C., Jiang, J.H., Yu, R.Q., 2012. Anal. Biochm. 423, 224–228.
Knowles, B.R., Wagner, P., Maclaughlin, S., Higgins, M.J., Molino, P.J., 2017. ACS Appl. Mater. Interfaces 9, 18584–18594.
Ladd, J., Taylor, A.D., Piliarik, M., Homola, J., Jiang, S., 2009. Anal. Bioanal. Chem. 393 (4), 1157–1163.
Lei, Y.M., Huang, W.X., Zhao, M., 2015. Anal. Chem. 87, 7787–7794.
Li, J., Yan, H., Wang, K., 2007a. Anal. Chem. 79, 1050–1056.
Li, L., Tao, L., Lubet, R.A., Steele, V.E., Pereira, M.A., 2007b. Carcinogenesis 28, 1499–1503.
Li, W., Liu, Z., Lin, H., Nie, Z., Chen, J., Xu, X., Yao, S., 2010. Anal. Chem. 82, 1935–1941.
Lin, H.Y., Chen, C.T., Chen, Y.C., 2006. Anal. Chem. 78 6873-6378.
Liu, N., Hui, N., Davis, J.J., Luo, X., 2018. ACS Sens. 3, 1210–1216.
Liu, X., Chen, M., Hou, T., 2014a. Biosens. Bioelectron. 54, 598–602 2014.
Liu, X., Huang, R., Su, R., Qi, W., Wang, L., He, Z., 2014b. ACS Appl. Mater. Interfaces 6, 13034–13042.
Luo, X., Li, Y., Zheng, J.B., Qi, H.L., Liang, Z.X., Ning, X.H., 2015. Chem. Commun. 51, 9487–9490.
Luo, X., Xu, Q., James, T., Davis, J.J., 2014. Anal. Chem. 86 (11), 5553–5558.
Mutze, K., Langer, R., Schumacher, F., Becker, K., Ott, K., Novotny, A., 2011. Eur. J. Cancer Care 47, 1817–1825.
Nowinski, A.K., Sun, F., White, A.D., Keefe, A.J., Jiang, S., 2012. J. Am. Chem. Soc. 134, 6000–6005.
Prime, K.L., Whitesides, G.M., 1991. Science 252, 1164–1167.
Ran, J., Wu, L., Zhang, Z., Xu, T., 2014. Prog. Polym. Sci. 39, 124–144.
Rauf, S., Zhang, L., Ali, A., Ahmad, J., Liu, Y., Li, J., 2017. Anal. Chem. 89, 13252–13260.
Rebeck, G.W., Samson, L., 1991. Bacteriol 173, 2068–2076.
Robertson, K.D., 2005. Nat. Rev. Genet. 6, 597–610.
Shao, K., Wang, B., Ye, S., Zuo, Y., Wu, L., Li, Q., 2016. Anal. Chem. 88, 8179–8187.
Sheehan, B.J., Dorman, C.J., 2010. Mol. Microbiol. 30, 91–105.
Sun, H., Ma, S., Li, Y., Qi, H., 2017. Sens. Actuators, B 244, 885–890.
Tian, T., Xiao, H., Long, Y., Zhang, X., Wang, S., Zhou, X., 2012. Chem. Commun. 48, 10031–10033.
Vaisocherová, H., Brynda, E., Homola, J., 2015. Anal. Bioanal. Chem. 407 (14), 3927–3953.
Van, S.B., Henikoff, S., 2000. Nat. Biotechnol. 18, 424–428.
Wang, G., Han, R., Su, X., Li, Y., Xu, G., Luo, X., 2017. Biosens. Bioelectron. 92, 396–401.
Wang, G., Su, X., Xu, Q., Xu, G., Lin, J., Luo, X., 2018. Biosens. Bioelectron. 101, 129–134.
Wang, X., Cui, M., Zhou, H., Zhang, S., 2015. Chem. Commun. 51, 13983–13985.
Wang, Y., He, X., Wang, K., Su, J., Chen, Z., Yan, G., Du, Y., 2013. Biosens. Bioelectron. 41, 238–243.
White, A.D., Nowinski, A.K., Huang, W.J., Keefe, A.J., Sun, F., Jiang, S.Y., 2012. Chem. Sci. 3, 3488–3494.
Wu, J.N., Han, H.J., Jin, Q., Li, Z.H., Li, H., Ji, J., 2017a. ACS Appl. Mater. Interfaces 9, 14596–14605.
Wu, L., Ding, F., Yin, W., Ma, J., Wang, B., Nie, A., 2017b. Anal. Chem. 89, 7578–7585.
Yang, Y., Liang, Y., Zhang, C., 2017. Anal. Chem. 89, 4055–4061.
Zeng, Y.P., Hu, J., Long, Y., Zhang, C.Y., 2013. Anal. Chem. 85, 6143–6150.
Zhao, Y.X., Chen, F., Wu, Y.Y., Dong, Y.H., Fan, C.H., 2013. Biosens. Bioelectron. 42, 56–61.
Zhao, Y., Chen, F., Lin, M., 2014. Biosens. Bioelectron. 54, 565–570.
Zhou, H., Han, T., Wei, Q., Zhang, S., 2016. Anal. Chem. 88, 2976–2983.